Int. J. Multiphase Flow Vol. 19, No. 6, pp. 1061–1076, 1993
Printed in Great Britain.
0301-9322/93 $6.00 + 0.00

FRICTION FACTOR AND HOLDUP STUDIES FOR LUBRICATED PIPELINING—I

EXPERIMENTS AND CORRELATIONS

M. S. ARNEY,[1] R. BAI,[1] E. GUEVARA,[2] D. D. JOSEPH[1] and K. LIU[3]
[1]Department of Aerospace Engineering and Mechanics, University of Minnesota, Minneapolis, MN 55455, U.S.A.
[2]INTEVEP S.A., San Tomé, Venezuela
[3]Deltac Corp., Plymouth, MN 55426, U.S.A.

(Received 15 July 1992; in revised form 20 July 1993)

Abstract—Results from new experiments on the lubricated pipelining of emulsified waxy crude oil and No. 6 fuel oil are presented and compared with other sources of literature. A correlation formula which estimates the holdup fraction is introduced and evaluated for all available experimental data. A simple theory is given which is based on the concentric core-annular flow model and leads to a Reynolds number and friction factor which reduce a large body of experimental data onto one curve; with the best results in the high Reynolds number flow regime.

Key Words: core, annular, flow, lubricated, pipeline, two-phase flow

INTRODUCTION

Water-lubricated pipelining is a method for transporting crude oil at low cost. The viscous oil forms a core that is surrounded and lubricated by a water annulus. Only the water contributes to the frictional losses in the pipe. The method leads to big savings in pumping power. A systematic approach is needed for design. In the late nineteenth century, the development of the Moody Chart involving the Reynolds number and the Fanning friction factor facilitated the design and development of single-fluid pipeline systems. Here, we try to extend this type of engineering analysis to lubricated pipelining.

A number of authors have, in fact, attempted such an application. Russel & Charles (1959) suggested a friction factor which is based on the superficial velocity of the water. This formulation did work for their particular problem, but could not be extended to other cases. Charles *et al.* (1961) developed a theory where the viscous core is treated as a solid "capsule". Later, Sinclair (1970) also developed a Reynolds number–friction factor correlation like that of Russel & Charles (1959) and applied it, with reasonable success, to his larger pipes. Oliemans (1986) did not try a Reynolds number–friction factor formulation; instead he analyzed the case of a very viscous, wavy, eccentric core and an annulus in laminar flow down a pipe. By balancing the buoyancy with lubrication forces he predicted the eccentricity of the core, and through numerical methods directly predicted the pressure drop. This method works well in the laminar case when the gap between the core and pipe are given and has the added advantage of using a model that is closer to reality. However, the model does not extend to the turbulent case, which is where most industrial processes operate.

Russel & Charles (1959) also published data for stratified flow and bubbly oil in water flow in a pipe using a low viscosity oil. Their work preceded the landmark paper of Charles *et al.* (1961) who showed results from three different oils and qualitatively similar results, which included a description and mapping of all the different flow regimes for oil-in-water flow through a pipe. But, they could not compare their results with other pipelines, since this data did not exist. Sinclair (1970) presented data from three different pipelines, but he did not do holdup measurements and used one constant input ratio for all of his experiments. Oliemans (1986) performed measurements on two different pipe sizes. There is also the work of Bai *et al.* (1992), which is the only experiment on a vertical pipeline.

The purpose of this paper is to introduce new data for further analysis and to offer a simple, reliable method using a Reynolds number and friction factor for the reduction of all data found in the literature resulting in a single master curve. In addition, an empirical formula which correlates all known holdup data is also given and compared with previous results. The formulas shown here are complete and sufficient for estimating the pressure drop in a core-annular flow process. The effectiveness of this technique is analyzed and discussed.

EXPERIMENTS ON WAXY CRUDE OIL AND NO. 6 FUEL OIL

To begin, experimental results are presented on the lubricated pipelining of waxy crude oil and No. 6 fuel oil with water. In spite of the potential usefulness of lubricated pipelining, a large database of even the simplest pressure drop vs flow rate and holdup vs flow rate data does not exist in the literature. Measurements of pressure drop vs flow rate and holdup vs flow rate are shown for waxy crude oil/water emulsion (a Bingham plastic) and No. 6 fuel oil (Newtonian) flowing in a 1.65 m long, 15.9 mm i.d. glass pipeline. Then, a comparison of some experimental results found in the literature is presented.

Description of the Apparatus

The apparatus is shown in figure 1. A screw-type positive displacement (Moyno) pump draws the oil from the supply tank and passes it through a Micro-Motion® Model C mass flow meter and feeds it to the center of a nozzle located at the head of the pipe. The flow rate of the oil is controlled either by varying the speed of the pump or by manipulating the feed and bypass valves. Water is drawn from a supply tank that is pressurized with compressed air, is passed through a filter and a rotameter and is pumped into the annulus of the nozzle. The flow rate is controlled with another gate valve. A centrifugal pump is placed on the water line and is used when needed to increase the water pressure. The temperatures of both the oil and water were monitored as they entered and exited the pipeline. No significant changes in temperature were observed.

The pipeline consists of three parts. The first part is used for flow development and visualization. Its purpose is to show the type of flow regime occurring in the pipeline. Glass pipe (15.9 mm i.d. and 6.35 m long) is used here since it is preferentially wetted by the transparent water rather than the opaque oil. To reduce the "lens" effect associated with the curved pipe, rectangular boxes filled with glycerol (a liquid which has an index of refraction that closely matches that of the glass)

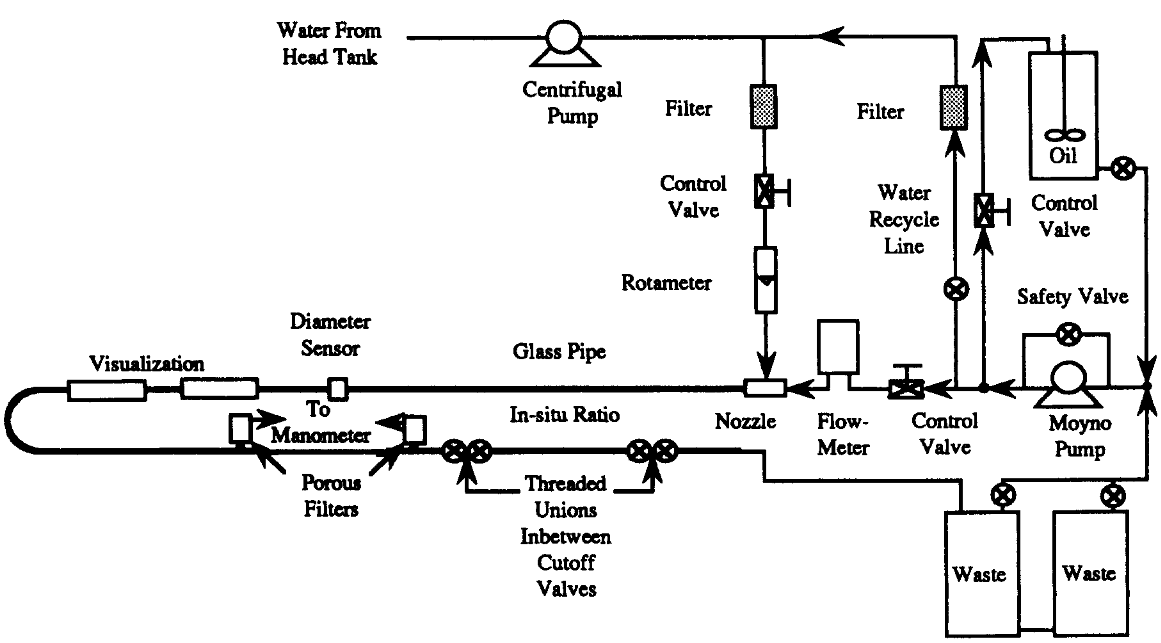

Figure 1. Pipeline diagram.

surround the outside of the pipe. Video-tapes of the flow were made with a Spin-Physics® SP2000 high-speed video system and still pictures were taken with a 35 mm camera.

The pressure drop is measured in the second part of the pipeline. A 2.16 m calming section is placed before the first pressure tap allowing the flow to develop. The two pressure taps located 1.42 m apart are each connected to a water manometer. To prevent fouling of the pressure lines, two large, very porous filters which absorb the oil but allow the water to pass are placed in the pressure lines just after the pressure taps.

Originally, the pressure drop and visualization sections were constructed from a transparent PVC pipe (15.7 mm i.d.) in order to take advantage of the material's greater ultimate strength, especially around the pressure taps. The pipeline was cleaned regularly with detergent and water. This method worked well with waxy crude oil; however, we were obliged to change to glass (15.9 i.d.) because No. 6 fuel oil very tenaciously adheres to the wall of the PVC pipe and promotes the formation of dangerous oil clots. Also, the fuel oil could not be cleaned from the pipe wall with detergent and water, but instead required the use of hazardous and environmentally unsafe petroleum solvents. No. 6 fuel oil does not readily wet glass and oil that stuck to the wall of the glass pipe could be removed by running clean water through the pipe.

The water volume fraction (also called the holdup volume fraction as defined [1] below) was measured in the third section of the pipe. This section is 1.47 m long and is a glass tube (15.9 mm i.d.) with two ball valves on each end. Each pair of ball valves is connected by a threaded coupling. To measure the holdup, the four ball valves are suddely closed and the oil pump is simultaneously switched off, stopping the flow. The pipe is then removed by unscrewing the couplings. Then, the contents of the pipe are emptied into a 200 ml graduated cylinder. The oil and water are allowed to separate in the graduated cylinders overnight, after which their volumes are measured. After each set of experiments, the oil and water separate in the waste tank and are pumped back to their respective feed tanks and reused.

Description of the Core Fluid

The waxy crude oil (density = 985 kg/m^3) is really a homogenized, stable emulsion of water in waxy crude oil. The viscosity of the pure crude oil was 6 P when the experiment was first started. After $1\frac{1}{2}$ years of use, the water and oil have formed a water-in-oil emulsion of approx. 70% water by weight. Before each experiment, the oil was mixed with a screwtype impeller which served to homogenize the oil/water emulsion. Figure 2, below, shows the behavior of the oil under constant stress. The measurement was done on a Rheometrics® Stress Rheometer using a 25 mm dia parallel plate and a 2 mm gap. The fluid shows a definite yield stress of approx. 400 Pa. After yielding, the fluid's viscosity, shown in figure 3, decreases monotonically to a value of 2000 P. It was not possible to get data for stresses greater than 1300 Pa since the fluid broke up under the higher stresses, i.e. the upper plate gave a large, sudden increase in rotation rate and the fluid separated into two parts, some sticking to the top plate, the rest sticking to the bottom plate. Due to the Bingham plastic nature of the crude oil, its interfacial tension with water could not be determined.

No. 6 fuel oil is a Newtonian fluid with a viscosity of 27 P. Its density of 0.989 g/cm^3 closely matches that of water. The interfacial tension between the oil and water is 26.3 dyn/cm.

Holdup Measurements

The holdup volume fraction H_w as a function of the input fraction C_w was measured for crude oil and No. 6 fuel oil and the values are shown in figure 4. C_w and H_w are defined, as in Oliemans (1986), to be

$$H_w = \frac{V_w}{V_o + V_w} \qquad [1]$$

and

$$C_w = \frac{Q_w}{Q_w + Q_o}, \qquad [2]$$

where $V_w = \pi(D_2^2 - D_1^2)L/4$ is the volume of water in the pipe, $V_o = \pi D_1^2 L/4$ is the volume of oil in the pipe, D_1 is the diameter of the core, D_2 is the diameter of the pipe, L is the pipe length, Q_w

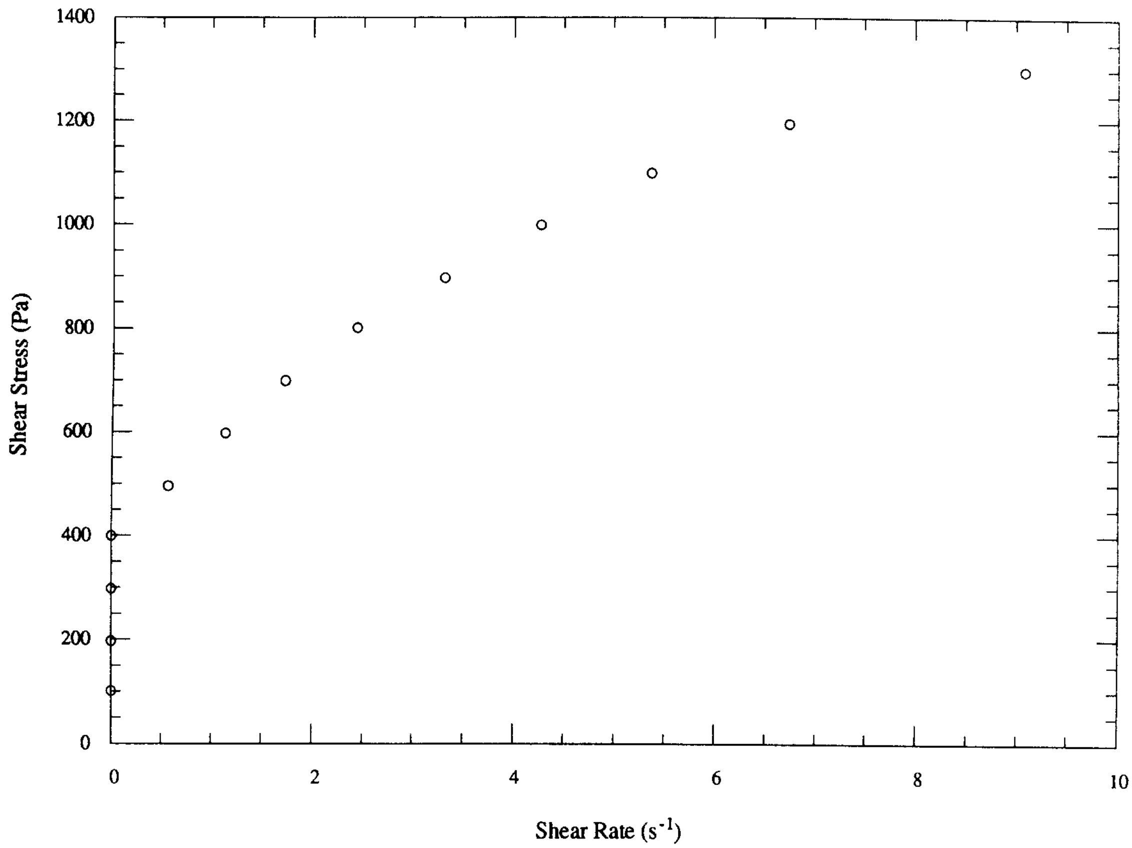

Figure 2. Stress vs strain curve for crude oil emulsified with 70 wt% water. The fluid has a yield stress of about 400 Pa.

is the volume flow rate of water and Q_o is the volume flow rate of oil. The most satisfactory reduction of holdup data was obtained using these two parameters. For the measurements shown in figure 4, superficial velocities varied between 0.061–0.65 m s^{-1} for water and 0.20–1.16 m s^{-1} for oil. H_w is consistently larger than C_w, indicating that the average velocity of the water annulus is slower than the average velocity of the oil core. Hence, it is said that the water is being held back. The slower water velocity must lead to a larger annulus thickness in order to satisfy the volume flow rate. Hence D_1 is reduced and H_w increased. Similar observations are made in Charles *et al.* (1961) and Bai *et al.* (1992).

The data for waxy crude oil shows more scatter than for No. 6 fuel oil. The possibility of experimental errors can be excluded since the same procedures were used for both oils. The scatter is most likely because the waxy crude oil is a Bingham plastic with a very high yield stress. The core diameter, in general, is determined by a balance of hydrodynamic forces, interfacial tension and internal stresses. A Newtonian fluid cannot support internal stresses without deforming; therefore for each oil and water input there will be a unique value of the core diameter which satisfies this balance of forces. A Bingham plastic on the other hand can support internal stresses without flow. In this case, the force balance can be satisfied by a *range* of core diameters and thus cannot be determined by the oil and water inputs alone. An extreme example of this is a solid rod in an airline whose diameter does not change irrespective of the air velocity, tube velocity, line diameter or other flow parameters.

Pressure Drop vs Flow Rate Curves

The pressure drop vs flow rate plots for waxy crude oil and No. 6 fuel oil are shown in figures 5–7. The procedure used to obtain this data is identical to that used by Charles *et al.* (1961) and Bai *et al.* (1992). In the first set of experiments, performed on waxy crude oil, the oil flow rate was held at the desired value while the water flow rate was varied and the pressure was measured.

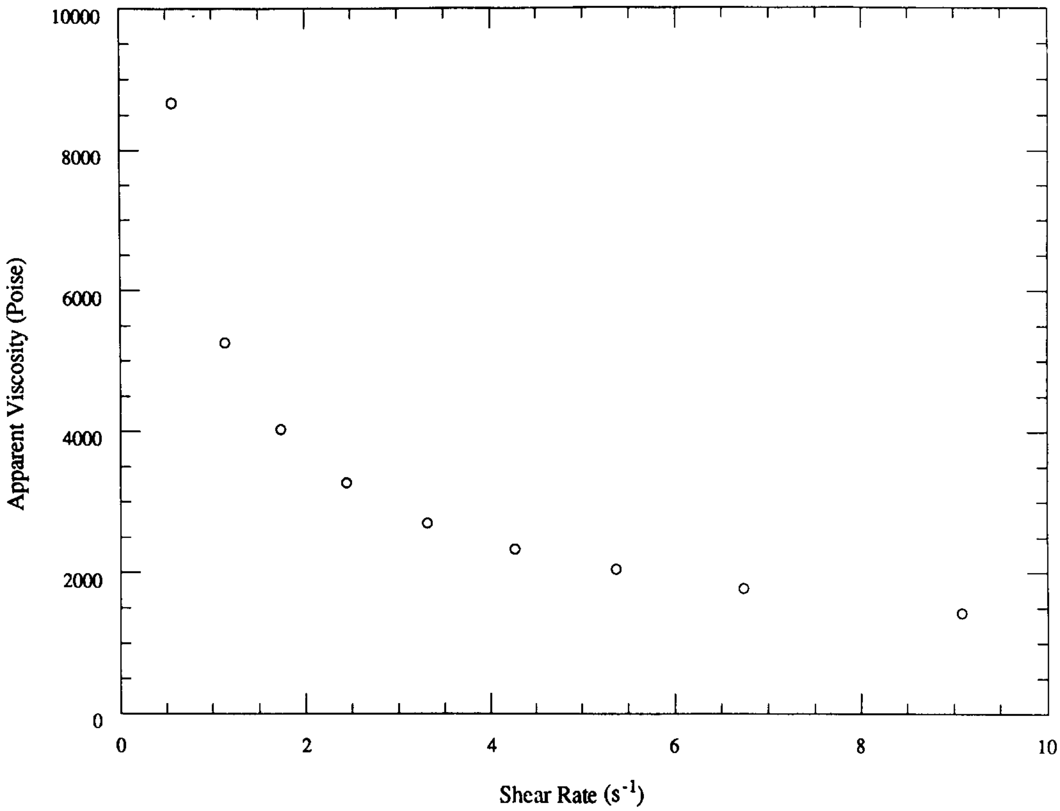

Figure 3. Apparent viscosity of emulsified crude oil. After yielding, the viscosity varies between 2000 and 9000 P.

The results are displayed in figure 5. In the next experiment, the water flow rate held constant while the crude oil flow rate was changed, and the results are displayed in figure 6. Lastly, the crude oil was replaced with No. 6 fuel oil, and pressure measurements were made for fixed oil flow rate and varied water flow rate; these results are shown in figure 7. All plots follow the convention of Charles *et al.* (1961). The reader should note that this convention defines the input ratio differently depending on the experiment: for figures 5 and 7, input ratio $= Q_w/Q_o$; for figure 6, input ratio $= Q_o/Q_w$. Flow charts showing the transition points to the various flow regimes are overlaid on figures 5 and 7. However, we observed a moderate amount of hysteresis around these transition points and their precision is approx. $\pm 5\%$.

These figures exhibit the same trends with more or less parallel curves no matter whether the oil input is fixed and the water input is varied, as in figures 5 and 7, or the water input is fixed and the oil input is varied, as in figure 6. These same trends can also be seen in Charles *et al.* (1961) and Bai *et al.* (1992), even though they used different pipe diameters, different oils and different flow configurations (Bai *et al.* use a *vertical* pipeline). This observation strongly suggests the possibility that all data can be reduced to a single master curve independent of pipeline geometry and weakly dependent on the core's material properties.

As in the study of Bai *et al.* (1992), we found that when the oil flow rate is held constant, there is an optimal water flow rate which minimizes the pressure gradient; at this flow rate either bamboo waves or disturbed core-annular flow is observed. The flow rate is called optimal because the product (oil) is being transported with the minimum of effort. However, care should be taken when operating in this flow region because if the water flow rate is too low the amount of water in the pipe is not sufficient to lubricate the core. In this case, the oil sticks to the wall of the pipe and forms a clot that constricts the flow. The oil and water still flow past the clot in a core-annular flow arrangement, but the core is very unstable; more oil peels off of the core and sticks to the pipe wall, thus propagating the clot [Bai *et al.* (1992) called this "chugging"]. The velocity of the oil and water rise, leading to an elevated pressure gradient and an even more unstable core. Over

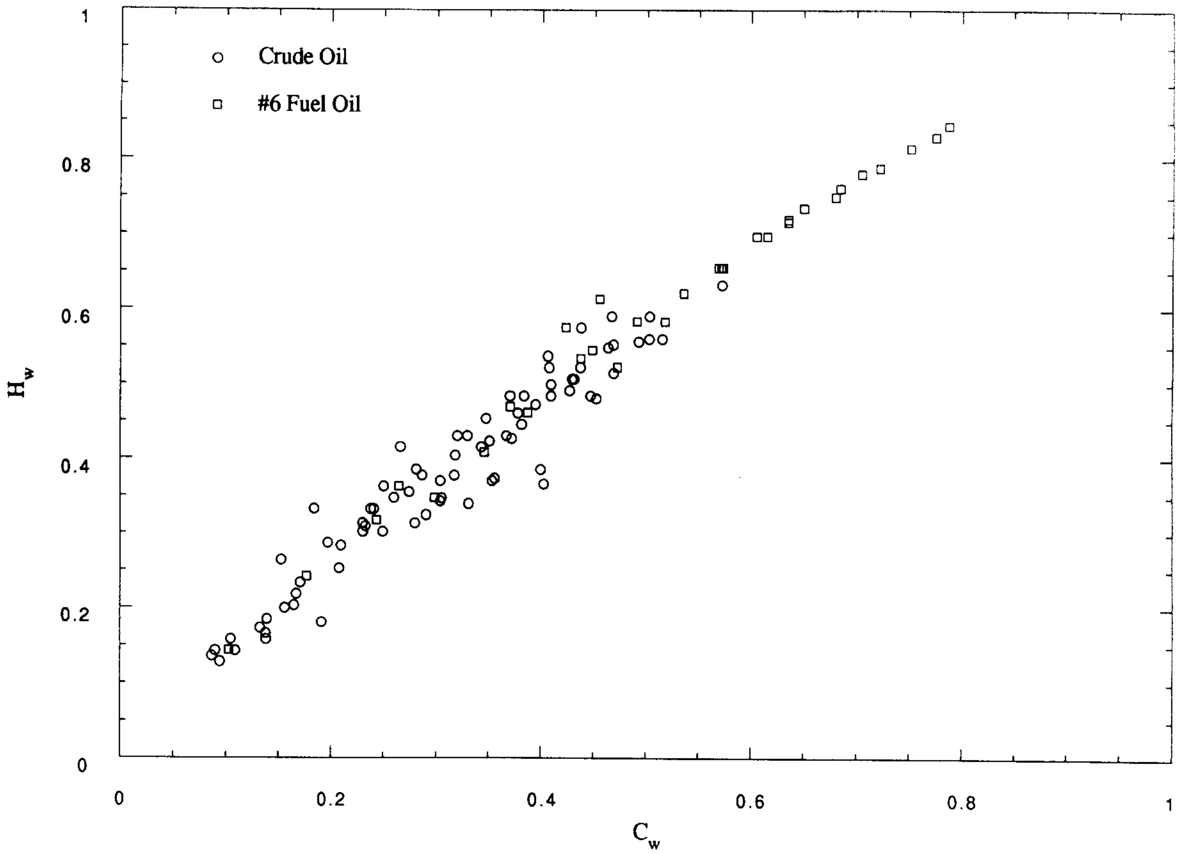

Figure 4. C_w vs H_w for waxy crude oil and No. 6 fuel oil.

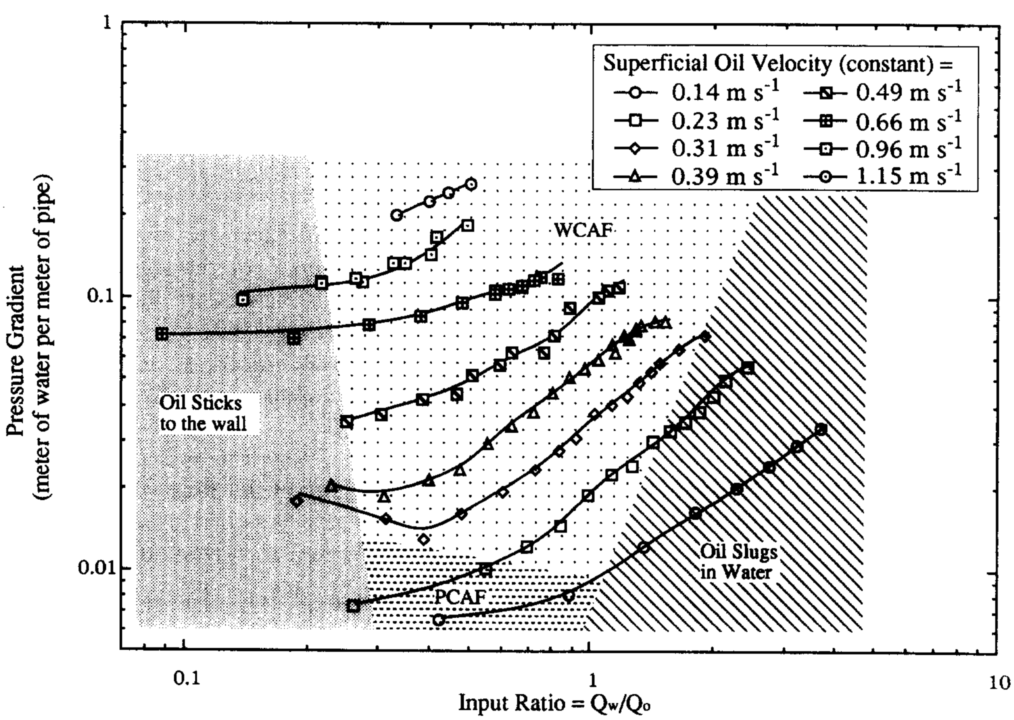

Figure 5. Pressure gradient vs input ratio for crude oil, with the oil flow rate held constant.

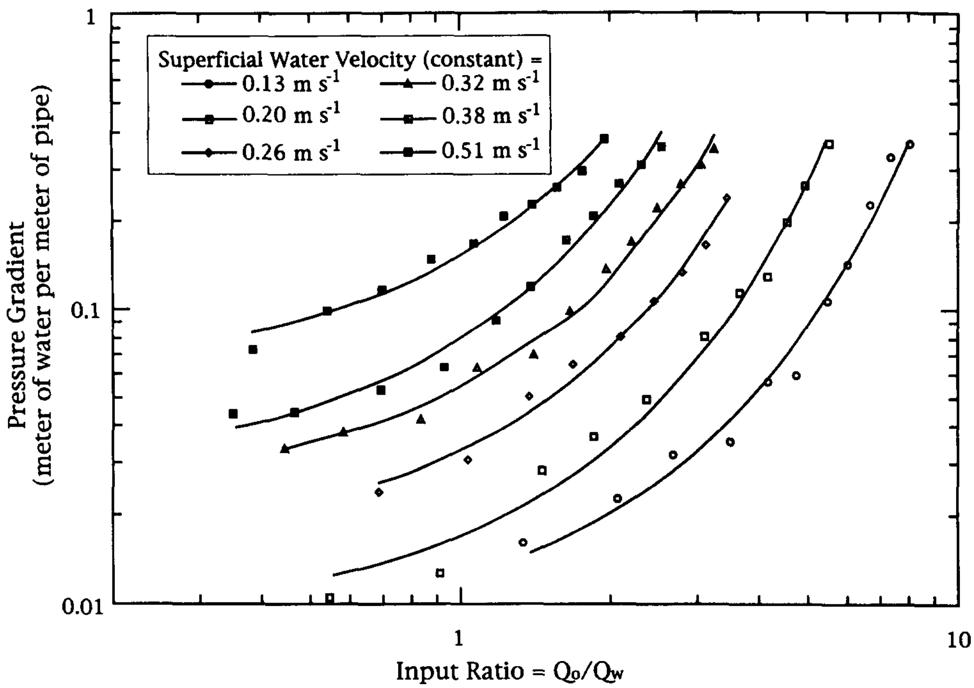

Figure 6. Pressure gradient vs input ratio for crude oil, with the water flow rate held constant.

time, if this situation is not corrected, the oil and water mix and form a catastrophic water-in-oil emulsion; a fluid which has a viscosity that is higher that the viscosity of the oil alone. The emulsion seizes the wall and the pressure gradient jumps dramatically.

In our pipeline, this situation could be detected easily by observing the pipe and monitoring the pressure. The problem could be corrected by greatly increasing the water flow rate or decreasing the oil flow rate. This action completely removed the oil from the hydrophilic glass pipeline, but

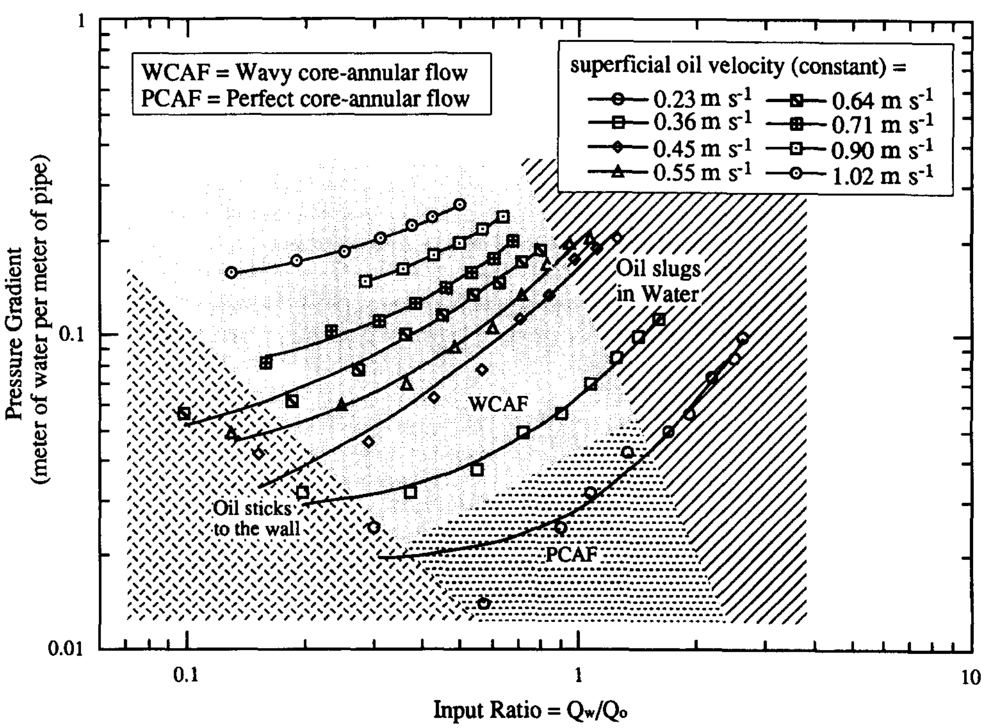

Figure 7. Pressure gradient vs input ratio for No. 6 fuel oil, with the oil flow rate held constant.

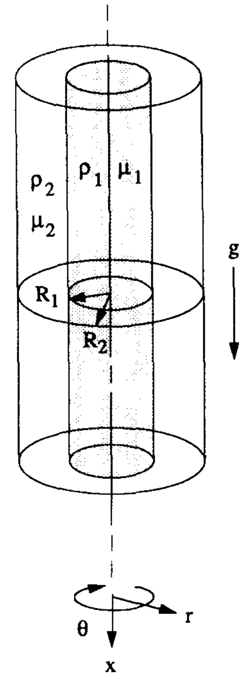

Figure 8. Core-annular flow.

was not completely effective with the hydrophobic PVC pipe. The fact that the oil is cleanly removed from the glass wall is also reported by Bai *et al.* (1992) and suggests that the problem of oil sticking to the wall can be controlled by using a pipe with hydrophilic walls.

Reynolds Number and Friction Factor

The equations for the Reynolds number and friction factor continue from equations presented in Bai *et al.* (1992). The Reynolds number and friction factor plots are a dimensionless expression of the pressure drop vs flow rate for the perfect core-annular flow shown in figure 8. The x-axis points in the direction of the flow (figure 8 shows down flow). The core has a density ρ_1, viscosity μ_1 and radius R_1 and is centrally located in a pipe of radius R_2. The core is surrounded by an annulus with density ρ_2 and viscosity $\mu_2 < \mu_1$. A vertical pipeline is used to demonstrate the effects of gravity. The velocity $W(r)\hat{\mathbf{e}}_z$ depends only on r and the Navier–Stokes equation reduces to

$$-\hat{P}' + \rho_l g + \mu_l\left(W_l'' + \frac{1}{r} W_l'\right) = 0, \qquad [3]$$

which holds for down flow (for the up flow equations, change the direction of the x-axis to point upwards and the sign of the gravity term to be negative) with $l = 1$ for the core, $0 < r < R_1$, and $l = 2$ for the annulus, $R_1 < r < R_2$, and

$$\frac{d\hat{P}_1}{dx} = \frac{d\hat{P}_2}{dx} = \hat{P}'$$

is one and the same constant pressure gradient, both in the core and annulus. The pressure gradient is given by $-\hat{P}' = [P_{\text{inlet}} - P_{\text{outlet}}]/L$, where L is the distance between the inlet and outlet and P_{inlet} and P_{outlet} are measured values of the pressure. Bai *et al.* (1992) noticed in their experiments that, in general, the value of R_1 was smaller in the up flow pipe than in the down flow pipe, meaning that the pressure gradient $\hat{P}'$ drives the flow and also compensates for a buoyancy overburden. We cannot use $\hat{P}'$ in developing correlation's of the pressure gradient with the mass flux because the buoyancy overburden is not found in horizontal flow. For this, we must first take away the part of $\hat{P}'$ which balances the overburden and find the dynamic pressure gradient p' which drives the flow and enters into the correlations with the mass flux. The removal of the overburden in a static fluid is easy, but in a moving fluid this removal requires an analysis associated with the composite (volume-averaged) density of the mixture:

$$\rho_c = (1-\eta^2)\rho_2 + \eta^2\rho_1, \qquad [4]$$

where

$$\eta = \frac{R_1}{R_2}.$$

The dynamic pressure p is then given by

$$\hat{P} = p + \rho_c g x.$$

Differentiating this with respect to x, adding $\rho_l g$, and rearranging, we then get:

$$-\hat{P}' + \rho_l g = -p' + (\rho_l - \rho_c)g. \qquad [5]$$

Using [4], the $(\rho_l - \rho_c)$ term becomes:

core
$$\rho_1 - \rho_c = (1-\eta^2)[\![\rho]\!] \qquad [6a]$$

and

annulus
$$\rho_2 - \rho_c = -\eta^2[\![\rho]\!], \qquad [6b]$$

where

$$[\![\rho]\!] = \rho_1 - \rho_2.$$

After substituting [5] and [6] into [3], the Navier–Stokes equations become:

core
$$-p' + (1-\eta^2)[\![\rho]\!]g + \mu_1\left(W'' + \frac{1}{r}W'\right) = 0, \quad 0 \leqslant r \leqslant R_1 \qquad [7a]$$

and

annulus
$$-p' - \eta^2[\![\rho]\!]g + \mu_2\left(W'' + \frac{1}{r}W'\right) = 0, \quad R_1 \leqslant r \leqslant R_2 \qquad [7b]$$

Equations [7a, b] show that core-annular flow in a vertical pipe depends on the density through the density difference and only through the density difference. These terms disappear entirely from the governing [7a, b] when the flow is all oil, $\eta = 1$, or all water, $\eta = 0$. Bai *et al.* (1992) developed a method to measure p' in a vertical pipeline which will not be given here.

The solution of [7a, b], along with the no-slip boundary conditions $W_1(R_1) = W_2(R_1)$, $\mu_1 W_1'(R_1) = \mu_2 W_2'(R_1)$ at $r = R_1$ and $W_2(R_2) = 0$, is given by Chen *et al.* (1990) as

$$W_1(r) = \frac{f_1}{4\mu_1}(R_1^2 - r^2) + \frac{f_2}{4\mu_2}(R_2^2 - R_1^2) + \frac{R_1^2[\![\rho]\!]g}{2\mu_2}\ln\frac{R_2}{R_1}, \qquad [8]$$

where

$$f_1 = -p' + (1-\eta^2)[\![\rho]\!]g \qquad [9a]$$

and

$$f_2 = -p' - \eta^2[\![\rho]\!]g, \qquad [9b]$$

and

$$W_2(r) = \frac{f_2}{4\mu_2}(R_2^2 - r^2) - \frac{R_1^2[\![\rho]\!]g}{2\mu_2}\ln\frac{r}{R_2}. \qquad [10]$$

The oil flow rate is given by

$$Q_1 = 2\pi \int_0^{R_1} r W_1(r)\,\mathrm{d}r$$

$$= 2\pi\left\{\frac{f_1}{16\mu_1}R_1^4 + \frac{f_2}{8\mu_2}(R_2^2R_1^2 - R_1^4) + \frac{R_1^4[\![\rho]\!]g}{4\mu_2}\ln\frac{R_2}{R_1}\right\}. \qquad [11]$$

The water flow rate is given by

$$Q_2 = 2\pi \int_{R_1}^{R_2} r W_2(r)\,\mathrm{d}r$$

$$= 2\pi\left\{\frac{f_2}{16\mu_2}(R_2^2 - R_1^2)^2 + \frac{[\![\rho]\!]g}{8\mu_2}\left(R_1^2R_2^2 + 2R_1^4\ln\frac{R_1}{R_2} - R_1^4\right)\right\}. \qquad [12]$$

When there is all oil in the pipe $R_1 = R_2$ and $Q_2 = 0, f_1 = p'$. When there is all water in the pipe $R_1 = 0$ and $Q_1 = 0, f_2 = -p'$. Hence in both cases

$$Q = -\frac{p'}{8\mu}\pi R_2^4. \qquad [13]$$

When $g = 0$, the case of matched densities studied by Charles *et al.* (1961), we have

$$Q_1 = -\frac{p'\pi R_1^4}{8\mu_1}\left[1 + 2\frac{\mu_1}{\mu_2}\left(\frac{R_2^2}{R_1^2} - 1\right)\right] \qquad [14]$$

and

$$Q_2 = \frac{-p'\pi}{8\mu_2}(R_2^2 - R_1^2)^2. \qquad [15]$$

Equations [11] and [12] can be combined to find the average velocity V:

$$V = \frac{Q_1 + Q_2}{\pi R_2^2} \qquad [16]$$

$$= \frac{[\eta^4(m-1)+1](-2p'R_2^2)}{16\mu_2} + \frac{(1-\eta^2)\eta^2[1+\eta^2(m-1)]}{16\mu_2}2R_2^2[\![\rho]\!]g \qquad [17]$$

where $m = \mu_2/\mu_1$ is the viscosity ratio. Equation [17] predicts the pressure drop vs flow rates for perfect, laminar core-annular flow.

An appropriate definition of the friction factor can be derived from a force balance over the entire pipe (figure 9):

$$\pi R_2^2(p_1 - p_2) = 2\pi R_2 L\tau_w, \qquad [18]$$

where τ_w is the shear stress on the wall. Hence

$$\Delta p = \frac{2L\tau_w}{R_2} \qquad [19]$$

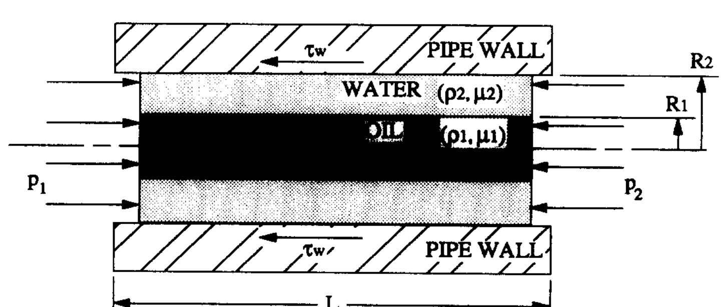

Figure 9. Force balance.

and

$$-p' = \frac{2\tau_w}{R_2}, \tag{20}$$

where $\Delta p = p_1 - p_2$ and p' is the dynamic pressure gradient $-p' = \Delta p/L$. The friction factor (resistance coefficient) λ, defined in the usual way [see, for example, Schlichting (1960, p. 505)], eliminates τ_w:

$$\frac{8\tau_w}{\rho_c V^2} = \lambda(\mathfrak{R}), \tag{21}$$

where ρ_c is the composite density [4], V is the average velocity, [16] and [17], and $\mathfrak{R}$ is a to-be-determined Reynolds number.

We next rearrange [17] so that the friction factor is on the LHS, with the remainder on the RHS;

$$\lambda = -p' \frac{2D_2}{\rho_c V^2} \tag{22a}$$

$$= \frac{64\mu_2}{D_2\rho_c V[1+\eta^4(m-1)]} - \frac{2[\![\rho]\!]gD_2(1-\eta^2)\eta^2[1+\eta^2(m-1)]}{\rho_c V^2[1+\eta^4(m-1)]} \tag{22b}$$

and

$$\lambda = \frac{64}{\mathfrak{R}} - B, \tag{23}$$

where $D_2 = 2R_2$ is the diameter of the pipe, $m = \mu_2/\mu_1$, $\rho_c(\eta)$ is the composite density [2],

$$\mathfrak{R} = \frac{\rho_c D_2 V}{\mu_2}[1+\eta^4(m-1)] \tag{24}$$

and

$$B = \frac{2[\![\rho]\!]gD_2(1-\eta^2)\eta^2[1+\eta^2(m-1)]}{\rho_c V^2[1+\eta^4(m-1)]}. \tag{25}$$

In a vertical pipe, if the flow is downward and $[\![\rho]\!] < 0$ then $B < 0$. For up flow, the signs of the two velocities and the pressure gradient change so that $-p' > 0$. In summary,

$$\lambda = \frac{64}{\mathfrak{R}} - B \quad \text{for down flow}$$

and

$$\lambda = \frac{64}{\mathfrak{R}} + B \quad \text{for up flow.}$$

Equation [22], which is plotted in figure 10 using typical values of ρ_1, ρ_2, μ_1, μ_2 and D_2, shows that the friction factor depends strongly on η, implying that for vertical flow the friction factor is affected by the diameter of the core through the buoyancy term B. The *maximum* friction factor occurs at about $\eta = 0.5$ or 0.6 for the down flow; for up flow, the *minimum* friction factor occurs around $\eta = 0.5$ or 0.6. When the Reynolds number or η increases, the friction factor will tend to $64/\mathfrak{R}$. If η decreases to zero, the friction factor will also tend to $64/\mathfrak{R}$. An accurate, reliable estimate of the core radius is therefore needed to predict the pressure drop.

INTRODUCTION OF LITERATURE SOURCES

The key fluid properties and pipeline dimensions from 12 different experimental arrangements of 5 different groups are shown in table 1. We include all data sources known to us with the exception of Russel & Charles (1959) because their data only featured stratified flow or bubbly oil-in-water flow. Bai *et al.* (1992) show results for vertical flow in both up and down flow. Sinclair (1970) shows results for the same oil, but three different pipeline diameters. Charles *et al.* (1961)

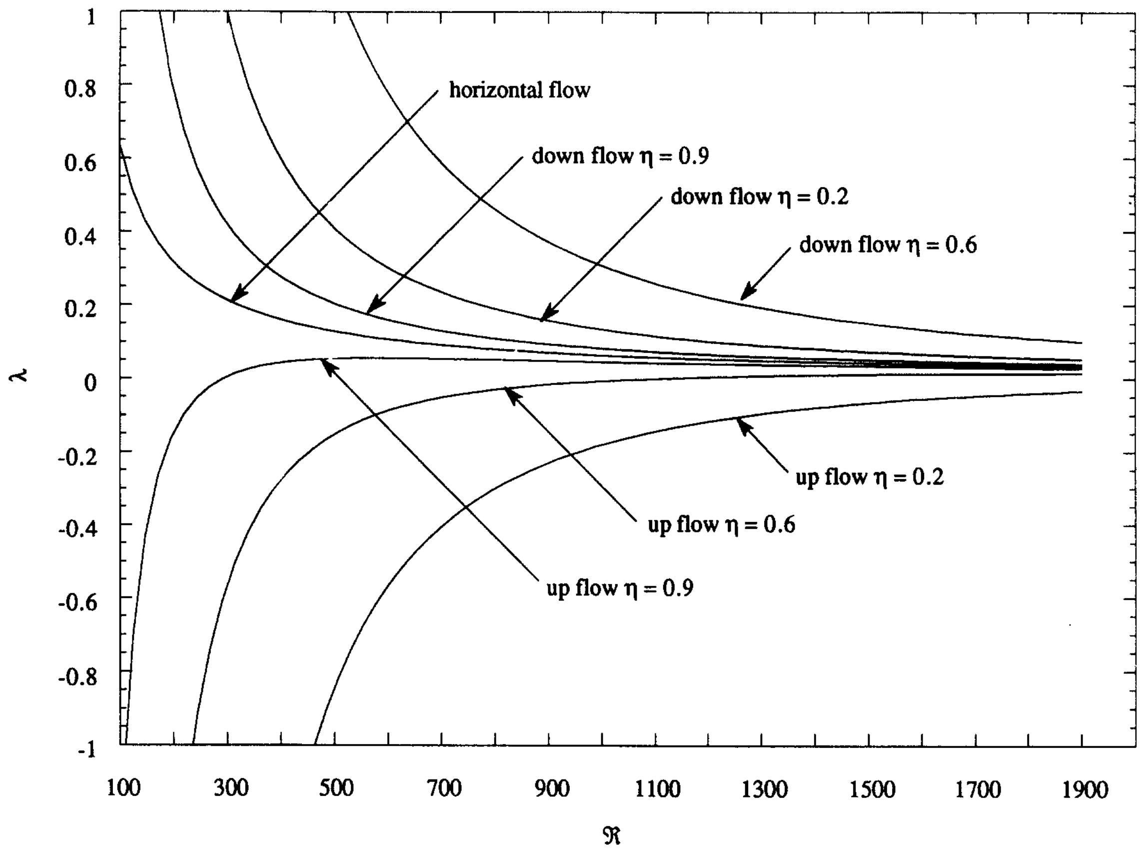

Figure 10. Theoretical friction factor, with $\rho_1 = 975\ \mathrm{kg/m^3}$, $\rho_2 = 1000\ \mathrm{kg/m^3}$, $\mu_1 = 900$ Pa-s, $\mu_2 = 0.001$ Pa-s and $D_2 = 0.0157$ m.

used the same pipeline, but with three different oils. Oliemans (1986) shows results from 2″ and 8″ pipelines. Also featured are data from an 8″ test line of INTEVEP, San Tomé, Venezuela using a bituminous crude and test data of Shell Oil Co., Houston, TX. The 12 different experimental arrangements are listed in table 1 with a wide variety of situations. Oils as thin as 6.03 cP and as thick as 1200 P are featured; pipe diameters range from 0.375″ to 8″ schedule 40 and pipe lengths range from as short as 56″ to as long as 24.24 miles.

Holdup Data

Figure 11 contains all the holdup data available in the literature. As with the holdup data for crude oil and No. 6 fuel oil shown above the holdup volume fraction is plotted as a function of the input fraction, achieving astonishingly good agreement among all the data sources. The points that show the most scatter, which are for the emulsified waxy crude oil and for the data from INTEVEP S.A., whose core fluid is non-Newtonian, but all the data for Newtonian oils show good agreement. The holdup data is fitted to the empirical formula

$$H_w = C_w[1 + 0.35(1 - C_w)], \qquad [26]$$

where the input fraction C_w and holdup H_w are defined in [1] and [2] above. A line corresponding to this formula is also shown in figure 11. This formula is really a modification of Oliemans (1986) equation [85]:

$$H_w = C_w[1 + 0.2(1 - C_w)^5], \qquad [27]$$

which is also shown. Equation [27] provides good insight for an empirical fit to the data, but [26] fits all the data more closely in light of the later sources of Bai et al. (1992) and the work presented here.

Table 1. Comparison of experiments

Author/group	Pipe length (m)	Pipe diameter (mm)	Core fluid	Annulus fluid	Oil density (kg/m^3)	Oil viscosity (Pa-s)	Water density (kg/m^3)	Water viscosity (Pa-s)	Symbol in figures 11 and 12
Bai *et al.* (1992)	2.29	9.53	20–30% Water in Mobile® cylinder oil	0.4% Sodium silicate in water	905	0.601	995	0.001	○
Charles *et al.* (1961)	7.32	26.4	20.6% Carbon tetrachloride in Marcol GX	Water	998	0.00629	998	0.00089	□
Charles *et al.* (1961)	7.32	26.4	18.7% Carbon tetrachloride in Wyrol J	Water	998	0.0168	998	0.00089	◇
Charles *et al.* (1961)	7.32	26.4	16.7 Carbon tetrachloride in Teresso 85	Water	998	0.063	998	0.00089	△
INTEVEP (Venezuela)	1009	203	Heavy crude oil	Water	990–1010	5–120	1000	0.001	⊙
Minnesota (No. 6 fuel oil)	19.8	15.9	No. 6 fuel oil	Water	995	2	998	0.00089	⧅
Minnesota (waxy crude oil)	19.8	15.7	27% Water in waxy crude oil emulsion	Water	985	>60	995	0.0009	⊞
Oliemans (1986)	8.99	50.8	"High viscosity oil"	Water	970	2.3	1000	0.00089	×
Oliemans (1986)	8.99	203	"High viscosity oil"	Water	970	2.3	1000	0.00089	+
Shell Oil (Houston, TX)	39,000	152	Crude oil	Water	992	12	1000	0.001	▲
Sinclair (1970)	15.2	19.1	Humble Fractol oil, water, emulsifier	Seawater	970	1	1030	0.001	◆
Sinclair (1970)	15.2	25.4	Humble Fractol oil, water, emulsifier	Seawater	970	1	1030	0.001	■
Sinclair (1970)	15.2	50.8	Humble Fractol oil, water, emulsifier	Seawater	970	1	1030	0.001	●

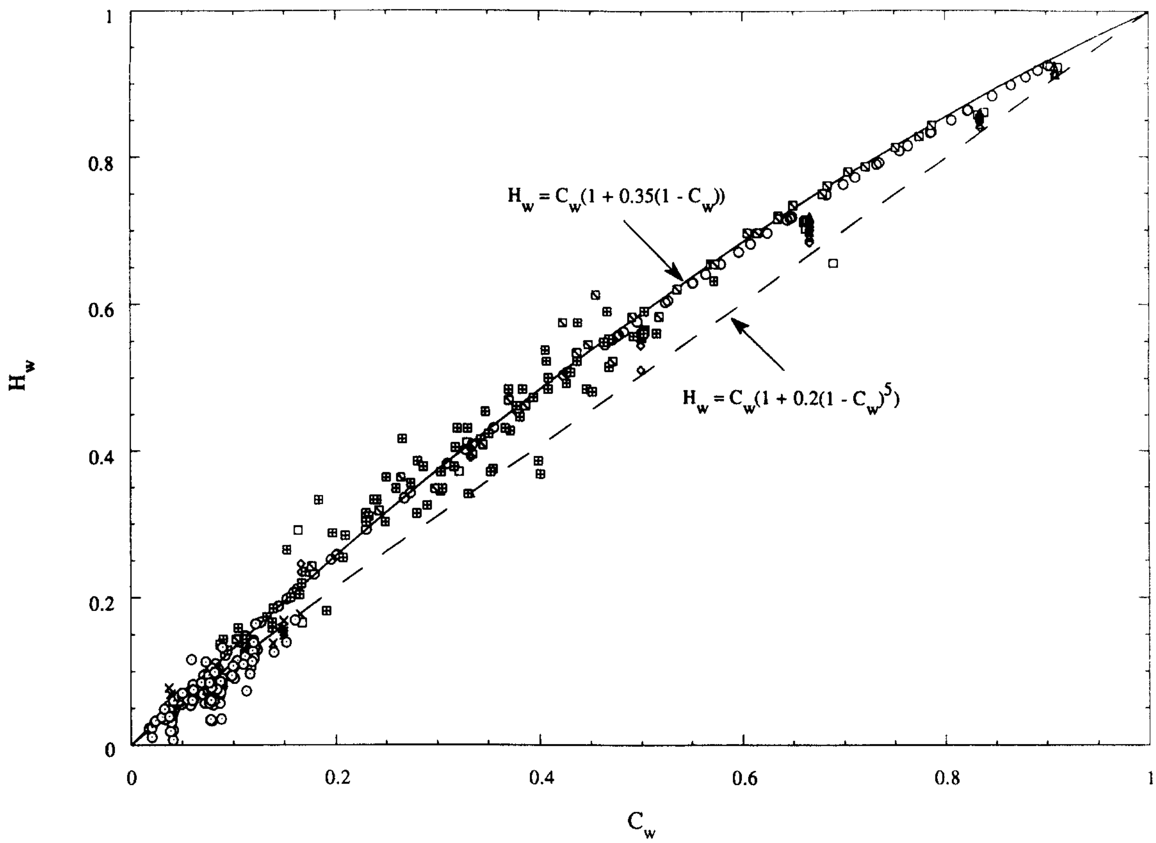

Figure 11. Holdup data for all known literature sources.

When the input fraction is known, [26] can be used to predict the holdup; then η can be calculated with

$$\eta = \sqrt{1 - H_w}, \qquad [27]$$

which can be used to compute the Reynolds number, [24].

Reynolds Number vs Friction Factor

Figure 12 is the result of applying [22a] and [24] to all of the pressure drop–flow rate data we have found in the literature. For comparison, lines corresponding to the theoretical formula for laminar flow,

$$\lambda = \frac{64}{\mathfrak{R}}, \qquad [28]$$

and the Blasius formula for turbulent flow,

$$\lambda = \frac{0.316}{\mathfrak{R}^{0.25}}, \qquad [29]$$

are also shown in figure 12. The Blasius formula fits the turbulent data fairly well and the reason has not been studied. This figure should be viewed with the following remarks in mind:

- Two sources, Sinclair (1970) and Shell Oil Co., Houston, did not give holdup data, so [26] was used to estimate the holdup and calculate the Reynolds number and friction factor.
- The data is fairly scattered for low Reynolds numbers. This should be expected because for slow flow rates, the core becomes very eccentric; gravity causes the core to rise to the top of the pipe. Therefore, the annulus thickness at the top of the

pipe is smaller causing the friction between the core and the wall to rise, hence there is an increased friction factor. This problem was studied by Oliemans (1986). Also, buoyancy forces in vertical flow cause changes in the friction factor (see the discussion above).

- Data from Charles *et al.* (1961) are taken from tables that are filed with the U.S. Library of Congress Photoduplication Service as well as figures 14, 16 and 18 of Charles *et al.* (1961). These tables show pressure gradients for all the flow regimes. However, only data corresponding to core flow and slug flow are used in our figure 12.
- Data from Oliemans (1986) was taken from his figures 17 (8″ pipeline) and 19 (2″ pipeline) and table 1 (2″ pipeline, turbulent flow). In his figures 17 and 19, the pressure gradients are reported in the form of a pressure reduction factor, which was first introduced by Russel & Charles (1959) and is defined as

$$\text{pressure reduction factor} = \frac{\Delta p_{ow}}{\Delta p_{so}},$$

where Δp_{ow} is the measured pressure drop and Δp_{so} is the pressure drop that would occur if the oil flows in the pipeline alone. The definition for Δp_{so} can be restated as

$$\Delta p_{so} = \frac{32\mu_o L V_o}{D^2},$$

where μ_o is the viscosity of the oil alone, V_o is the superficial velocity of the oil, L is the pipe length and D is the pipe diameter, which were all stated explicitly in the previously mentioned figures. The pressure gradients calculated in this manner from Oliemans' (1986) 8″ pipeline (data from his figure 17) are consistently

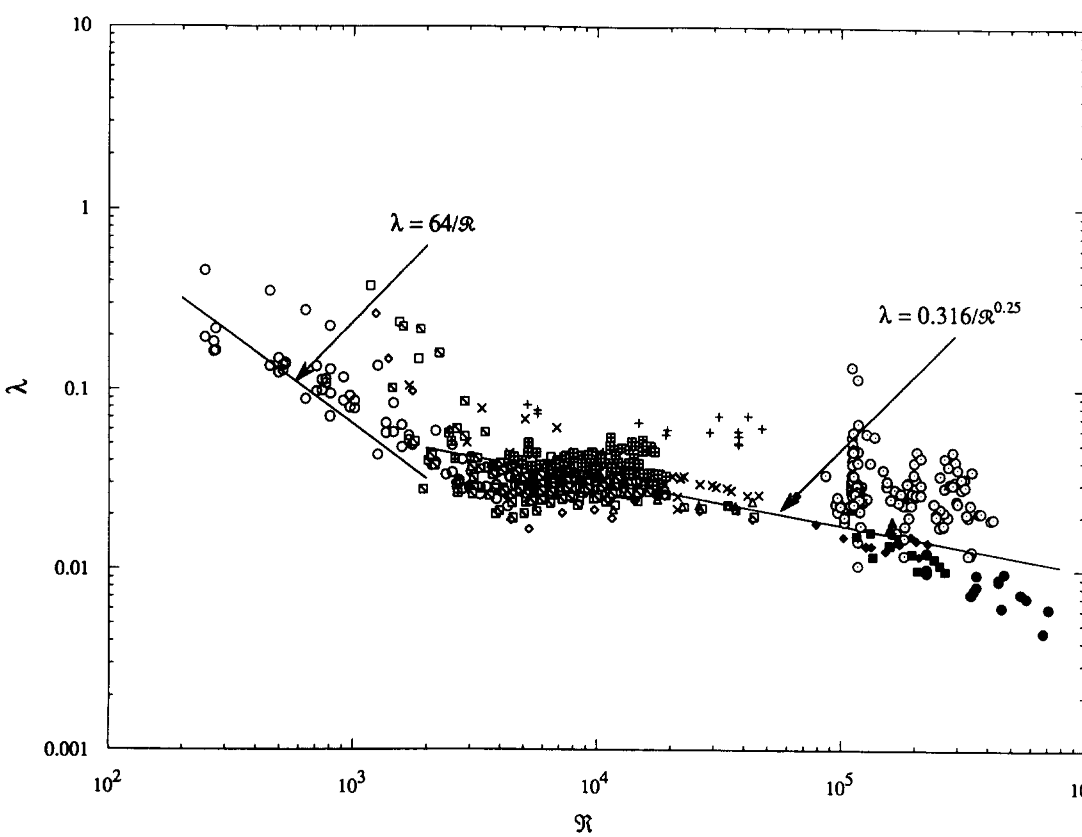

Figure 12. Reynolds numbers [24] vs friction factor [22a] for all known literature data.

two times higher than the data from the rest of the literature sources. This data is from a joint project between Oliemans and INTEVEP S.A. (Venezuela). Through communication with INTEVEP S.A., we have learned that the high pressure values were due to fouling of the pipe walls.

SUMMARY AND DISCUSSION

This paper can be summarized as follows:

- The results of pressure drop vs flow rate and holdup vs flow rate measurements for water-lubricated pipelining of emulsified waxy crude oil and No. 6 fuel oil are reported and are seen to be similar to previous work on lubricated pipelining.
- A theory which is based on concentric cylindrical core-annular flow is developed and yields simple Reynolds number and friction factor formulas ([22a] and [24]).
- Holdup fraction data for wide variety of experiments that are found in the literature are shown (figure 11) and an empirical equation ([26]) is given which closely fits all the sources of data. This formula can be used to estimate the diameter ratio for use in the Reynolds number.
- Pressure drop vs flow rate data is reduced using the Reynolds number and friction factor; these results are shown in figure 12. The data shows considerable scatter at low Reynolds numbers, but is very successful in reducing high Reynolds number data to a single master curve.

The technique we have presented provides some insight into the reasons for the frictional losses for core-annular flow: the skin friction caused by the lubricant shearing against the wall contributes to most of the frictional losses. This technique's main failure is that it does not account for other effects which serve to increase the frictional losses such as a wavy core, an eccentric core or the presence of bends, elbows, tees and other common fittings. The Reynolds number and friction factor are reasonably consistent when the pipe wall is clean. When the oil sticks to the wall the pressure drop increases, producing a corresponding rise in the friction factor. Therefore, excessive oil sticking to the wall will be indicated by an elevated friction factor.

Acknowledgements—This work was supported by grants from the ARO (Mathematics), INTEVEP S.A. (Venezuela) and the National Science Foundation. We gratefully acknowledge Professor C. W. Macosco of the Department of Chemical Engineering and Material Science, University of Minnesota, for the rheometer facilities and David Hultman for constructing an excellent pipeline.

REFERENCES

BAI, R., CHEN, K. & JOSEPH, D. D. 1992 Lubricated pipelining stability of core-annular flow, Part 5. Experiments and comparison with theory. *J. Fluid Mech.* **240,** 97–142.

CHEN, K., BAI, R. & JOSEPH, D. D. 1990 Lubricated pipelining, Part 3. Stability of core-annular flow in vertical pipes. *J. Fluid Mech.* **214,** 251–286.

CHARLES, M. E., GOVIER, G. W. & HODGSON, G. W. 1961. The horizontal pipeline flow of equal density oil–water mixtures. *Can. J. Chem. Engng* **39,** 27–36.

GOVIER, G. W. & AZIZ, K. 1972 *The Flow of Complex Mixtures in Pipes.* Van Nostrand Reinhold, New York.

OLIEMANS, R. V. A. 1986 *The Lubricating-film Model for Core-annular Flow.* Ph.D. Thesis, Technische Hogeschool Delft. Delft University Press, The Netherlands.

RUSSEL, T. W. F. & CHARLES, M. E. 1959 The effect of the less viscous liquid in the laminar flow of two immiscible liquids. *Can. J. Chem. Engng* **37,** 18–24.

SCHLICHTING, H. 1960 *Boundary Layer Theory.* Pergamon Press, New York.

SINCLAIR, A. R. 1970 Rheology of viscous fracturing fluids. *J. Pet. Technol.* **June,** 711–719.